ERDC MSRC

Major Shared Resource Center

ERDC MSRC/PET TR/00-38

# The Effect of the Wave Propagation Scheme on SWAN Nearshore Wave Predictions

by

Stephen F. Wornom
David J.S. Welsh
Keith W. Bedford

12 November 2000

01h00301

**Work funded by the DoD High Performance Computing Modernization Program ERDC Major Shared Resource Center through**

Programming Environment and Training (PET)

Supported by Contract Number: DAHC94-96-C0002
CSC Nichols

# Year 5 PET Report

# The Effect of the Wave Propagation Scheme on SWAN Nearshore Wave Predictions

Stephen F. Wornom*, David J. S. Welsh, Keith W. Bedford
Department of Civil Engineering and Geodetic Science
The Ohio State University

November 12, 2000

*ERDC MSRC PET onsite CWO academic lead

The Effect of Wave Propagation Scheme on SWAN Nearshore Wave Predictions

Topic: Nearshore Wave Predictions

Authors
Stephen F. Wornom, Research Scientist
U.S. Army Engineer Research and Development Center
ATTN: CEERD-IH-C Dr. Stephen Wornom
3909 Halls Ferry Road
Vicksburg, MS 39180-619
address all correspondence to this author

Tel: 601-634-4663
Fax: 601-634-3808
e-mail: wornomsf@wes.hpc.mil

David J. S. Welsh, Research Scientist
Department of Civil and Environmental Engineering and Geodetic Science
The Ohio State University
2070 Neil Avenue
Columbus,Ohio 43210

Tel: 614-292-6919
Tel: 614-292-3780
e-mail: welsh.1@superior.eng.ohio-state.edu

Keith W. Bedford, Professor and Chair
Department of Civil and Environmental Engineering and Geodetic Science
The Ohio State University
2070 Neil Avenue
Columbus,Ohio 43210

Tel: 614-292-3808
Tel: 614-292-3780
e-mail: bedford.1@osu.edu

# The Effect of the Wave Propagation Scheme on SWAN Nearshore Wave Predictions

**Abstract**

The application of wave modeling codes to predict nearshore wave conditions typically involve computations on multiple nests starting with a large coarse-grid ocean nest ending with a find-grid nearshore mesh. The nests are computed sequentially with each nest run creating the boundary spectra needed to drive the computation on the next finest mesh. The larger nests usually cover large regions of the ocean surface requiring spherical wave propagation to account for the effect of curvature of the earth to avoid errors in the wave predictions. As the size of the nests becomes smaller, the differences between a spherical grid and a Cartesian grid for the same nest become smaller and the wave modeler can often choose to use either spherical wave propagation or Cartesian wave propagation; the assumption being that as the nest size diminishes the differences in the computed results are small. This assumption was brought into question by a recent study of Wornom et al. [9], using the WAM code. That study found, the surprising result, that the Cartesian wave propagation results were more accurate than the spherical wave propagation results for their relatively large (2°x2°, approximately 222 km x 222 km) test zone. At the time of that study, another code was not available to numerically cross-check their finding. The purpose of this study was to test the spherical and Cartesian wave propagation schemes in the new release of the SWAN code (version 40.11) to determine their effect on nearshore wave predictions and verify the finding of the study of Wornom et al. [9]. The test case used in this study and the study of Wornom et al. [9] was a simulation of 1995 Hurricane Luis for which test data was available. The test site is located in the Atlantic Ocean along the outer banks of North Carolina and the coast of Virginia comprising five test sites. This study found that the computational results obtained using spherical wave propagation were more accurate than the results obtained with Cartesian wave propagation. Thus the observations of Wornom et al. [9] suggest possible coding issues in the WAM code, which become apparent in the nearshore zone, need to be examined.

Keywords: SWAN, nearshore wave prediction, 1995 Hurricane Luis, spherical wave propagation, Cartesian wave propagation

# 1 Introduction

Accurate prediction of nearshore wave conditions remains one of the major challenges in ocean modeling. In the nearshore zone, finite-depth effects like bottom friction, shoaling, and refraction play an important role and must be modeled accurately as they are of paramount importance in environmental impact studies involving erosion and sediment transport. Accurate predictions of the nearshore wave conditions is equally important in naval navigation into harbors and in landing operations.

The application of wave modeling codes to predict nearshore wave conditions typically involves computations on multiple nests of increasing mesh resolution. The nests are computed in a sequential manner starting with the largest nest. During the computation of each nest, the boundary spectra needed to drive the computation on the next finest mesh are saved. The larger nests may cover large regions of the ocean surface and the waves must be propagated on a sphere to account for the effect of curvature of the earth to avoid large errors in the predictions. For coastal and nearshore regions, smaller nests with higher mesh resolution are used. As the size of the nests becomes smaller, the differences between a spherical grid and a Cartesian grid for the same nest become smaller and the wave modeler has the option to use either spherical wave propagation or Cartesian wave propagation; the assumption being that as the size of the nest becomes small, the differences in the computational results are small.

In a recent study, Wornom et al. [9] examined the effect of the wave propagation scheme on the accuracy of nearshore wave predictions using the WAM code, which permits the user to select either spherical or Cartesian wave propagation. The study of Wornom et al. [9] found the surprising result that Cartesian wave propagation was more accurate than spherical wave propagation in their coastal and nearshore zone, which was relatively large grid ($2°$x$2°$, approximately 222 km x 222 km). The reason why the Cartesian wave propagation results were more accurate than the spherical wave propagation results was not determined. However, it was suggested that the reason might be related to the fact that the wave-action transport equation is divergence-free in Cartesian coordinates, but not in spherical coordinates. At the time of the study by Wornom et al. [9], only Cartesian wave propagation was available in the SWAN code, thus it was not possible to cross-check the WAM results with the SWAN code. With the release of v40.11 of the SWAN code, a similar study is now possible.

The purpose of this study was to apply the v40.11 of the SWAN code to the same test case used in the study of Wornom et al. [9] to study the effect of spherical and Cartesian wave propagation on the accuracy of the nearshore wave predictions. The test case is the same as used in the study of Wornom et al. [9], which involves a simulation of wind-wave activity during 1995 Hurricane Luis for which NOAA buoy and station data was available, as well as data from the U. S. Army Field Research Facility at Duck, NC. A comparison of the results from wave modeling codes with the wave observations permits evaluation of the codes indicating where certain models should or should not be applied, as well as bringing to light deficiencies in the physical models and their implementation. In the study of Wornom et al. [9], the comparison discovered the abnormally discussed above. Those observations merit further investigation. In contrast to the study of Wornom et al. [9], this study found that, the significant wave heights are more accurately predicted with the SWAN code when Cartesian wave propagation is used.

### 1.1 Description of the SWAN code

The SWAN code is a third generation wave model, which computes spectra of random short-crested wind-generated waves. SWAN accounts for the following basic physics:

- Wave propagation in time and space
- Wave generation by wind
- Shoaling and refraction due to depth
- Shoaling and refraction due to current
- Whitecapping and bottom friction
- Quadruplet wave-wave interactions

The SWAN code contains formulations for two physical processes not present in the WAM code: depth-induced wave-breaking and triad wave-wave interaction. These processes can play an important role for nearshore calculations and are the main reasons why the SWAN code is coupled with the WAM code in nearshore regions (see Wornom et al. [10]). In this study, only the same options as used in the WAM study (Wornom et al. [9]), were included.

SWAN solves a spectral wave-action transport equation shown here for the Cartesian wave propagation scheme.

$$\frac{\partial}{\partial t}\hat{E} + \frac{\partial}{\partial x}(c_x \hat{E}) + \frac{\partial}{\partial y}(c_y \hat{E}) + \frac{\partial}{\partial \sigma}(c_\sigma \hat{E}) + \frac{\partial}{\partial \theta}(c_\theta \hat{E}) = S/\sigma \tag{1}$$

where

$$S = S_{in} + S_{nl} + S_{wc} + S_{bf} + S_{dib} \tag{2}$$

and

| | |
|---|---|
| $\hat{E}(x,y,\sigma,\theta,t)$ | = wave action density spectrum |
| $\sigma$ | = relative frequency |
| $\theta$ | = wave direction |
| $S_{in}(\sigma,\theta)$ | = wind input |
| $S_{nl}(\sigma,\theta)$ | = non-linear wave-wave interaction |
| $S_{wc}(\sigma,\theta)$ | = dissipation due to whitecapping |
| $S_{bf}(\sigma,\theta)$ | = dissipation due to bottom friction |
| $S_{dib}(\sigma,\theta)$ | = depth-induced breaking |
| $c_x,\ c_y$ | = propagation velocities in Cartesian space |

SWAN uses the wave action density spectrum, $\hat{E}$, rather than the energy density spectrum, $E$, because in the presence of currents, the wave action density spectrum is conserved whereas the energy density spectrum is not. They are related through the relation

$$\hat{E} = E/\sigma \tag{3}$$

SWAN solves the spectral wave-action transport equation mesh using a fully implicit upwind scheme in geographical space. For the first time, SWAN users may choose spherical or Cartesian wave propagation. To the authors knowledge, this present work is the first study to compare both options. In directional and frequency space, the level of accuracy and diffusion can be selected by the user. The implicit scheme used in geographical space is unconditionally stable and thus avoids numerical instabilities. The time-step selection is designed to accurately capture the unsteady physics rather than to maintain numerical stability. In many cases this leads to smaller CPU time requirements. The details of the SWAN code are given by Booij et al. [1] and Ris et al. [8]. The SWAN code and the SWAN USER MANUAL [7] can be downloaded from the SWAN Web site (http://www.swan.ct.tudelft.nl).

### 1.2 Nested grid structure

Four nests were used in the present study. The nests are referred to as the "basin" (30-minute resolution, 135x120 cells), "region" (15-minute resolution, 120x96 cells), "subregion 1 (sub1)" (5-minute resolution, 84x120 cells), and "subregion 2 (sub2)" (5/4-minute resolution; 96x96 cells), moving from coarser to finer resolution. Table 1 gives information concerning the different nests used. WAM was run on the first three nests. The approximate mesh sizes are also given in Table 1. SWAN was run on the sub2 nest. The sub2 nest covers two degrees by two degrees, which is close to the limit where a Cartesian grid can be expected to produce accurate results owing to the curvature of the Earth.

**Table 1** Nest data

| nest level | max/min lon. (deg) | max/min lat. (deg) | resol. (min) | approx. mesh size (km) |
|---|---|---|---|---|
| basin | 345/277.5 | 70/10 | 30 | 54.7 km |
| region | 308/278 | 48/24 | 15 | 25.4 km |
| sub1 | 290/283 | 41/31 | 5 | 7.9 km |
| sub2 | 286/284 | 37/35 | 5/4 | 1.9 km |

The length of the sub2 nest sides, the mesh sizes, and the number of cells were: 182.0 km x 222.2 km, 5/4-minute resolution, 96x96 cells. The boundary condition spectra for the sub2 nest were obtained from the WAM run on the sub1 nest.

## 1.3 Mesh generation

**Cartesian grids**-In the SWAN code, the user supplies the length of the sides (in meters) of the computational grid and the number of cells in each direction. For the bathymetry and wind fields, the user supplies the spatial step size and the number of cells. The longitude and latitude of the southwest corner point must also be given. When using the WAM/SWAN interface, the following relations (not given in the SWAN USER Manual) must be used to convert the WAM nest defined in degrees to a SWAN nest defined in meters; otherwise, the WAM boundary spectra will be incorrectly placed on the SWAN mesh. The SWAN grid node spacings and lengths of the sides of the computational grid must be generated using the equations

$$\Delta x = F * \Delta longitude_d * \beta \tag{4}$$

and

$$\Delta y = F * \Delta latitude_d \tag{5}$$

where

$$\beta = cos(\frac{\pi}{180} * latitude_d) \tag{6}$$

and

$$F = \frac{Earth's\ circumference\ at\ the\ equator\ (meters)}{360} \tag{7}$$

where the subscript "d" denotes degrees. The Earth's circumference at the equator was taken as 40,000,000 meters. The factor $\beta$ accounts for the variation with latitude of the length (in meters) of a fixed increment of longitude (in degrees) due to the Earth's curvature.

**Spherical grids**- For the spherical grid, the user supplies the maximum and minimum values and the step size in the longitude and latitude directions in degrees.

These data are given in Table 1. On the sub2 nest, the Cartesian wave propagation option present in the WAM code was used.

### 1.4 Model couplings

Table 2 shows the the different coupled deployments of the WAM and SWAN codes used in this study. The WAM and SWAN runs on the different nests are coupled to WAM (or SWAN) through the boundary spectra, that were created by a previous coarse-grid WAM run.

**Table 2** Types of coupling

| Nest level | Type of coupling | Propagation scheme |
|---|---|---|
| basin | none | spherical |
| region | WAM-WAM | spherical |
| sub1 | WAM-WAM | spherical |
| sub2 | SWAN-WAM | Cartesian |
| sub2 | SWAN-WAM | spherical |

During the basin computation, predicted wave spectra are interpolated to the boundaries of the region and saved. Likewise, during the computations for the region, spectra are interpolated to the boundaries of subregion sub1 and saved; a similar procedure is followed for the sub2 nest. The boundary condition spectra, the winds, and the bathymetry drive the computations for the different nests.

## 2 Input and evaluation data

### 2.1 Bathymetry

The bathymetry data for the basin and region were supplied by Jensen [3]. The bathymetry for the sub1, and sub2 nests was downloaded from the Naval Oceanographic Office (NAVO) variable resolution gridded bathymetry database (DBDBV) [6].

### 2.2 Hindcast wind fields

The hindcast wind fields used to drive the WAM and SWAN computations nests were provided by Jensen[3]. The method used to generate the wind data is described by Cox et al. [2]. The wind fields are defined on the basin nest, which has a 30-minute mesh resolution and are interpolated to the region and subregion nests using bilinear surface interpolation.

## 3 SWAN deployment

The test sites are located in the Atlantic Ocean, along the outer banks of North Carolina and the coast of Virginia. The SWAN and WAM computations are compared with data from two NOAA C-MAN stations, one NOAA buoy, and two FRF test sites located at Duck, NC. These sites were selected because data were available for the September 1995 test period. Table 3 gives the latitude and longitude coordinates for the test sites and their approximate mean water depths. The water depths for NOAA buoy 44014 and the FRF 8-m array were taken from the NOAA and FRF Web sites. The water depths for NOAA stations chlv2 and dnsl2 were provided by Knoll [4]. The water depth for the FRF buoy wr630 was supplied by Long [5]. The test locations and bathymetry are shown in Figure 1, where Chesapeake Bay is indicated as "C. Bay," Albemarle Sound as "A. Sound," and Pamlico Sound as "P. Sound." Water depth contours less than 50 meters are shown. NOAA buoy 44014 and test station dsln7 are situated on the edge of the continental shelf; beyond the shelf the water depth increases rapidly to 3000-4000 m. NOAA buoy wr630 is located 4 km offshore, and the FRF 8-m array is 900 m offshore.

**Table 3** Test site data

| Test site | latitude | longitude | 360 + longitude | water depth, m |
|---|---|---|---|---|
| NOAA buoy 44014 | 36.5831 N | -74.8336 W | 285.1664 | 47.5 |
| NOAA station dsln7 | 35.1533 N | -75.2967 W | 284.7033 | 19.0 |
| NOAA station chlv2 | 36.9050 N | -75.7133 W | 284.2867 | 11.6 |
| FRF buoy wr630 | 36.1681 N | -75.6999 W | 284.3001 | 17.1 |
| FRF 8-m array | 36.1906 N | -75.7434 W | 284.2566 | 8.0 |

The WAM and SWAN calculations were made using 25 frequencies and 24 directions with the frequencies logarithmically spaced from 1/30 Hz to 1.1 Hz. The water depths are assumed to be the mean values. Currents and tidal effects were not considered in this study.

## 4 Test case: Hurricane Luis

The path of the eye of Hurricane Luis is indicated by the curving white line in Figure 2, which shows the WAM significant wave height contours for the region nest on 95/09/10, 0 UTC; this date approximately corresponds to the peak of the storm as measured at NOAA buoy 44014. The different WAM nests used can be seen in Figure 2. At the top right of Figure 2, the date and hour of the wave contours are shown; the state of Florida can be recognized in the lower left corner of the region nest. The coordinates used to plot the hurricane eye path shown in Figure 2 were obtained from the NOAA web site (http://www.nhc.noaa.gov/1995luis.html) and were not taken from the wind fields used to drive the wave simulations.

Figure 3 shows the significant wave height contours for the sub2 nest at 95/09/10, 0 UTC which is the nest used to evaluate the effect of the spherical and Cartesian propagation schemes. Also shown are the five test locations and an additional nest which was not used in this study. Overlaying the NOAA data on contour plots of the wind speed computed from the hindcast wind fields (see below) served to validate that the eye of the hurricane deduced from wind speed and significant wave height contour plots was consistent with the NOAA web site data.

Table 4 summarizes the types of measurements available at the different sites, using the indicated notations for significant wave height (Hmo), peak wave period (Tmax), and mean wave direction ($\theta_{mean}$).

**Table 4** Availability of data

| Instrument ID | location | Hmo | $\theta_{mean}$ | Tmax |
|---|---|---|---|---|
| NOAA buoy 44014 | Virginia Beach, VA | yes | yes | yes |
| NOAA station chlv2 | Chesapeake Light, VA | yes | no | yes |
| NOAA station dsln7 | Diamond Shls. Light, NC | yes | no | yes |
| FRF buoy wr630 | Duck, NC | yes | no | yes |
| FRF 8-m array | Duck, NC | yes | yes | yes |

## 5 Evaluation methods

The computational results from the SWAN runs were examined based on the difference between the calculated values and the instrument measurements using root-mean-square (rms) norms. Biases in the computations relative to the instrument measurements are also examined. These are computed using the ratios $\Delta H$ defined as:

$$\Delta H = H_c - H_d \tag{8}$$

where $H$ takes on the values of significant wave height, peak wave period, and mean wave direction and the subscripts "c" and "d" denote "computed" and "data" values. The root-mean-square norm (rms) and the bias are defined as:

$$rms(H) = \sqrt{\frac{1}{N}\sum_{i=1}^{N}(\Delta H_i)^2}, \tag{9}$$

$$bias(H) = \frac{1}{N}\sum_{i=1}^{N}\Delta H_i, \tag{10}$$

where "N" is the number of evaluation points.

The simulation period for this study was 95/08/29, 0 UTC to 95/09/13, 0 UTC. The evaluation period was taken as the 10-day period from 95/09/03, 0 UTC to 95/09/13, 0 UTC; the model spin-up portion of the simulation was not, therefore, used for evaluation purposes.

## 6 Discussion of results

The effect of the wave propagation method on the significant wave height is given in Table 5. It can be seen in Table 5, which shows that the rms and bias values for the period up to Sept. 10th, that the SWAN spherical propagation hindcasts are more accurate than the Cartesian hindcasts at all five test sites with the sole exception being the NOAA station chlv2 where the Cartesian rms value is slightly lower than the spherical rms value.

**Table 5** Comparison of rms and bias values

| | rms, significant wave height, m | | |
|---|---|---|---|
| test site | spherical | Cartesian | accuracy bias |
| NOAA 44014 | 0.634 | 0.642 | spherical |
| NOAA dsln7 | 0.554 | 0.605 | spherical |
| NOAA chlv2 | 0.156 | 0.150 | Cartesian |
| FRF wr630 | 0.274 | 0.324 | spherical |
| FRF 8-m array | 0.146 | 0.161 | spherical |
| | bias, significant wave height, m | | |
| buoy | spherical | Cartesian | accuracy bias |
| NOAA 44014 | -0.359 | -0.399 | spherical |
| NOAA dsln7 | -0.426 | -0.509 | spherical |
| NOAA chlv2 | -0.045 | -0.052 | spherical |
| FRF wr630 | -0.132 | -0.176 | spherical |
| FRF 8-m array | -0.076 | -0.089 | spherical |

## 7 Conclusions

The effect of the wave propagation method on nearshore wave prediction has been examined using version 40.11 of the SWAN code. In version 40.11, the user can choose, for the first time, to use spherical or Cartesian wave propagation.

The motivation for this study was a previous study by Wornom et al. [9], who examined the effect of the wave propagation scheme on the accuracy of nearshore wave predictions using the WAM code. The study of Wornom et al. [10] found the surprising result that Cartesian wave propagation was more accurate than spherical wave propagation for their relatively large test grid ($2°$x$2°$, approximately 222 km x 222 km). The reason why the WAM Cartesian wave propagation results were more accurate than the WAM spherical wave propagation results was not determined. Wornom et al. [10] proposed that the reason may be related to the fact that the WAM wave-action transport equation is divergence-free in Cartesian coordinates, but not in spherical coordinates. At the time of the study by Wornom et al. [9], only the Cartesian wave propagation was available in the SWAN code so it was not possible to cross-check the WAM results with the SWAN code. With the release of v40.11 of the SWAN code, this became possible and motivated this study.

The test case used in this study and the study of Wornom et al. [10] was a simulation of 1995 Hurricane Luis for which test data was available. The nest used to evaluate the propagation schemes was a relatively large test grid ($2°$x$2°$, approximately 222 km x 222 km) located in the Atlantic Ocean along the outer banks of North Carolina and the coast of Virginia comprising five test sites. This study found that the SWAN computations made with spherical wave propagation were more accurate than the results obtained with Cartesian wave propagation. In light of these findings, further study is needed to assertain the discrepancies between the nearshore wave predictions of the WAM and SWAN codes when Cartesian and spherical wave propagation is used.

# 8 Acknowledgement

This work was supported in part by a grant of HPC time from the DoD HPC Modernization Program at the U.S. Army Engineer Research and Development Center Major Shared Resource Center in Vicksburg, Mississippi. The authors would like to thank Dr. Robert Jensen of the Coastal and Hydraulics Laboratory at the U. S. Army Engineer Research and Development Center for suggesting and supporting this study, and for providing the Hurricane Luis wind fields.

The wind fields used in this study were developed by Oceanweather, Inc., under funding by the Atmospheric Environment Service, Canada.

# References

[1] Booij, N., Ris, R. C., and Holthuijsen, L. H., 1999, "A third-generation wave model for coastal regions, Part I, Model description and validation," *J. Geoph. Research* 104, C4, 7649-7666.

[2] Cox, A. T., Greenwood, J. A., Cardone, V. J., and Swail, V. R., 1995, "An Interactive Objective Kinematic Analysis System," 4th International Workshop on Wave Hindcasting and Forecasting, Banff, Alberta.

[3] Jensen, Robert, DoD Lead scientist, Global and Regional Wind-Wave Modeling Coastal and Hydraulic Laboratory, U.S. Army Engineer Research and Development Center, Vicksburg, Mississippi

[4] Knoll, D., National Oceanographic Data Center, Silver Spring, MD., 2000

[5] Long, C.E., Research Oceanographer, U.S. Army Field Research Facility, Duck, N.C., 2000

[6] http://128.160.23.42/dbdbv/dbdbv.html.

[7] Holthuijsen, L. H., Booij, N., Ris, R.C., Haagsma, IJ. G., Kieftenburg, A.T.M.M., and Padilla-Hernandes, R., 1999, "SWAN version 40.01 USER MANUAL,"

[8] Ris, R. C., Booij, N., and Holthuijsen, L. H., 1999, "A third-generation wave model for coastal regions, Part II, Verification," *J. Geoph. Research*, 104, C4, 7667-7681.

[9] Wornom, S. F., and Welsh, J. S., "A Comparison of the SWAN and WAM Wave Model for Nearshore Wave Predictions", ERDC MSRC/PET TR/00-16, April 18, 2000, Vicksburg, MS http://www.wes.hpc.mil/pet/tech_reports/reports/pdf/tr_00_16.pdf

[10] Wornom, S. F., Welsh, J. S., and Bedford, K. W., "On Coupling the SWAN and WAM Wave Models for Accurate Nearshore Wave Predictions", ERDC MSRC/PET TR/00-31, August 1, 2000, Vicksburg, MS http://www.wes.hpc.mil/pet/tech_reports/reports/pdf/tr_00_31.pdf

**Figure 1** Bathymetry and Location of buoys

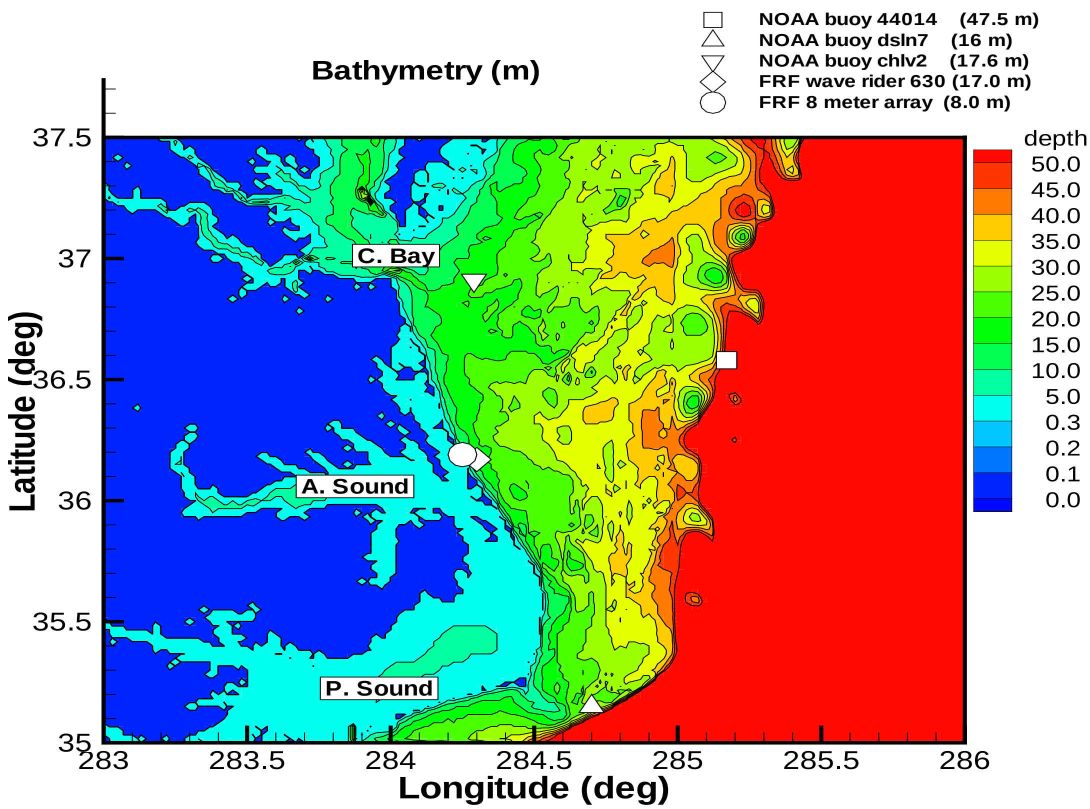

**Figure 2** Region: WAM significant wave height: 95/09/10, 0 UTC

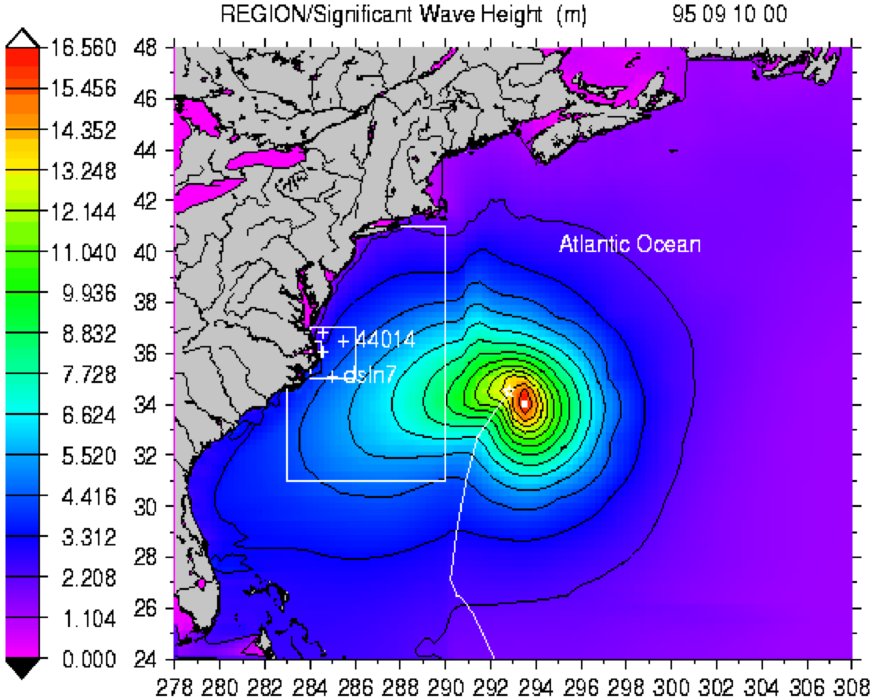


**Figure 3** sub2: WAM significant wave height: 95/09/10, 0 UTC

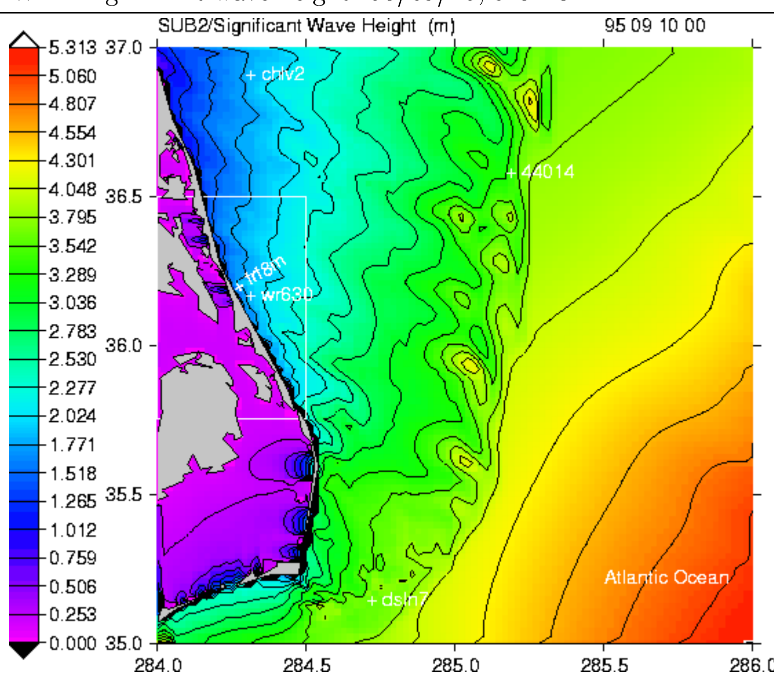

**Figure 4** The effect of wave propagation method on Hmo: NOAA buoy 44014

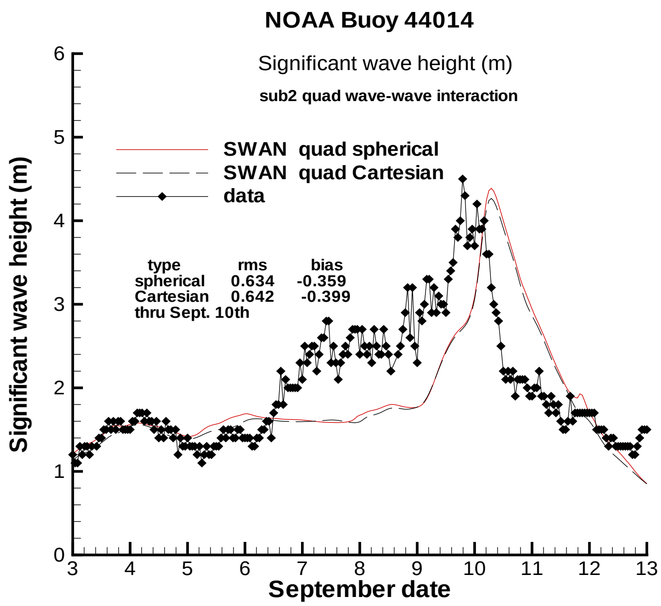


**Figure 5** The effect of wave propagation method on Hmo: NOAA station dsln7

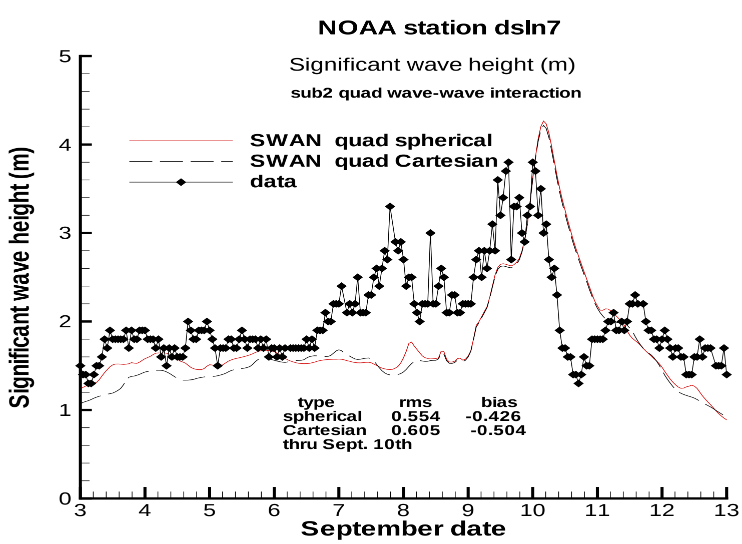

**Figure 6** The effect of wave propagation method on Hmo: NOAA station CHLV2

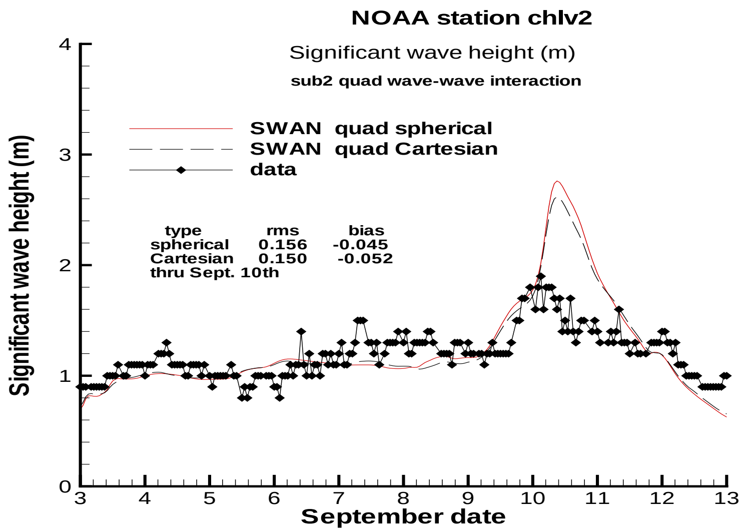


**Figure 7** WAM: the effect of spherical and Cartesian wave propagation on Hmo: FRF 8-m array

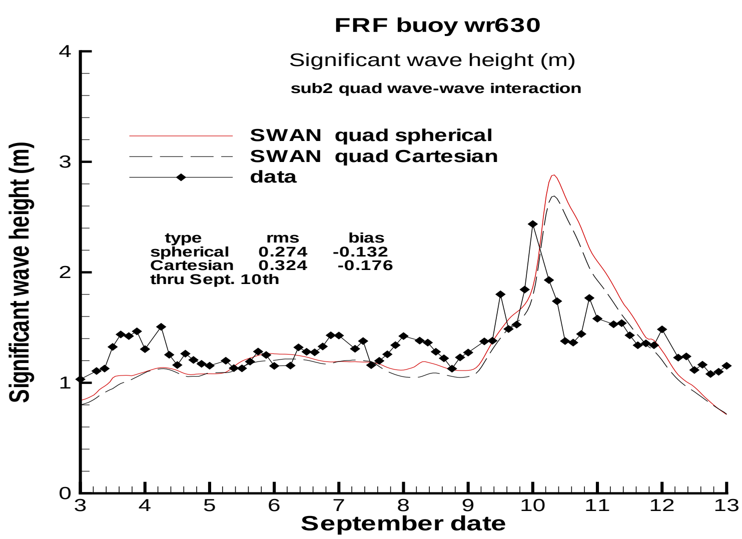

**Figure 8** WAM: the effect of spherical and Cartesian wave propagation on Hmo: FRF 8-m array